International Journal of Modern Physics B
Vol. 30, No. 13 (2016) 1642003 (7 pages)

DOI: 10.1142/S0217979216420030

World Scientific
www.worldscientific.com

# Tuning $g$-factor of electrons through spin–orbit coupling in GaAs/AlGaAs conical quantum dots

Sanjay Prabhakar*,‡ and Roderick Melnik*,†

*The MS2 Discovery Interdisciplinary Research Institute,
$M^2NeT$ Laboratory, Wilfrid Laurier University,
Waterloo, N2L 3C5 ON, Canada
†BCAM-Basque Center for Applied Mathematics,
E48009 Bilbao, Spain
*sprabhakar@wlu.com

Received 16 December 2015
Accepted 29 February 2016
Published 23 March 2016

We investigate band structures of GaAs/$Al_{0.3}Ga_{0.7}As$ three-dimensional conical quantum dots (QDs). In particular, we explore the influence of the Rashba and Dresselhaus spin–orbit couplings in the variation of effective $g$-factor of electrons in such QDs. We demonstrate that the interplay between the Rashba and Dresselhaus spin–orbit couplings can provide further insight into underlying physical phenomena and assist in the design of quantum logic gates for the application in spintronic devices.

*Keywords*: Conical semiconductor quantum dots; spin–orbit coupling; $g$-factor of electrons.

PACS numbers: 41.20.Jb, 03.65.Pm, 71.10.Pm

## 1. Introduction

There is a growing interest in making the next generation optoelectronic devices from semiconductor quantum dots (QDs) for application in spintronics, and applications in quantum computing and quantum information processing.[1–4] A better understanding of $g$-factor of electrons plays a key role in the design of III–V semiconductor optoelectronic devices.[5–8] The experimental studies in QDs confirm that the manipulation of $g$-factor of electrons by spin–orbit coupling is important for the design of spintronics logic and other devices.[9] The spin–orbit coupling consists of the Rashba[11] and the linear Dresselhaus[12] terms that arise from structural inversion asymmetry along the growth direction and the bulk inversion asymmetry of

‡Corresponding author.

the crystal lattice.[1,2,13] The variation in the $g$-factor of electrons with electric and magnetic fields in gated III–V semiconductor QDs with the Rashba and Dresselhaus spin–orbit couplings were explored in Refs. 5, 13–16. In-plane anisotropy induced by the gate potential also influences the effective Landé $g$-factor of electrons in QDs.[5,9,21] In this paper, we consider three-dimensional GaAs/$Al_{0.3}Ga_{0.7}$As conical QDs that are epitaxially formed due to lattice mismatch at the heterojunction. We study the variation in the $g$-factor of electrons with electric and magnetic fields for the pure Rashba, pure Dresselhaus and mixed cases. Here, we show that the penetration of electron $g$-factor from GaAs region to the AlGaAs region can be achieved with the externally applied electric field along $z$-direction. This provides the variation in the effective $g$-factor of electrons that can be utilized to design quantum switches for application in spintronics devices.

The rest of the paper is organized as follows: in Sec. 2, we formulate a theoretical model of three-dimensional semiconductor QDs in the presence of externally applied electric and magnetic fields, accounting for both the Rashba and Dresselhaus spin–orbit couplings. In Sec. 3, we provide details of the diagonalization technique used for finding the eigenvalues and eigenstates of electrons in QDs and highlights main features of the associated computational methodology. In Sec. 4, we analyze the effective $g$-factor of electrons with several control parameters such as electric and magnetic fields as well as the lateral size of QDs. Finally, in Sec. 5, we summarize our results.

## 2. Theoretical Model

We consider an epitaxially formed GaAs/$Al_{0.3}Ga_{0.7}$As QD. In the presence of a magnetic field applied along $z$-direction, we write the total Hamiltonian of such a QD as:[1,10,13,17,22]

$$H = H_0 + H_R + H_D\,, \tag{1}$$

where $H_R$ and $H_D$ are the Hamiltonian associated with the Rashba and Dresselhaus spin–orbit couplings and

$$H_0 = \frac{\mathbf{P}^2}{2m} + V(x,y,z) + eE_z z + \frac{1}{2} g_o \mu_B \sigma_z B\,, \tag{2}$$

where $\mathbf{P} = \mathbf{p} + e\mathbf{A}$ is the kinetic momentum operator, $\mathbf{p} = -i\hbar(\partial_x, \partial_y, \partial_z)$ is the canonical momentum operator, $\mathbf{A} = B(-y, x, 0)$ is the vector potential, $m$ is the effective mass of the electron in the conduction band, $\mu_B$ is the Bohr magneton and $\boldsymbol{\sigma} = (\sigma_x, \sigma_y, \sigma_z)$ are the Pauli spin matrices. Also, $V(x,y,z)$ is the confinement potential which is zero in the GaAs region and 0.3 eV in the barrier material and $E_z$ is the applied external field along $z$-direction. The Hamiltonians associated with the Rashba and Dresselhaus spin–orbit couplings can be written as[11–13]

$$H_R = \frac{\alpha_R}{\hbar}(\sigma_x P_y - \sigma_y P_x)\,, \tag{3}$$

$$H_D = \frac{\alpha_D}{\hbar}(-\sigma_x P_x + \sigma_y P_y)\,, \tag{4}$$

where the strengths of the Rashba and Dresselhaus spin–orbit couplings are characterized by the parameters $\alpha_R$ and $\alpha_D$. They are given by

$$\alpha_R = \gamma_R eE\,, \quad \alpha_D = 0.78\gamma_D \left(\frac{2me}{\hbar^2}\right)^{2/3} E^{2/3}\,, \tag{5}$$

where $\gamma_R$ and $\gamma_D$ are the Rashba and Dresselhaus coefficients. Now, we write $H|\Psi\rangle = \varepsilon|\Psi\rangle$ in terms of two coupled eigenvalue problem in the basis states $|\psi_1\rangle$ and $|\psi_2\rangle$ as

$$\begin{aligned}\Big[ &-\frac{\hbar^2}{2m}(\partial_x^2+\partial_y^2+\partial_z^2)+\frac{1}{8}m\omega_c^2(x^2+y^2)-\frac{i\hbar\omega_c}{2}(-y\partial_x+x\partial_y)+V(x,y,z)\\ &+eE_z z+\frac{1}{2}g_0\mu_B B\sigma_z\Big]|\psi_1\rangle+\Big[\alpha_R eE_z\Big\{\partial_x-i\partial_y+\frac{m\omega_c}{2\hbar}(x-iy)\Big\},\\ &+\alpha_D\Big\{i\partial_x-\partial_y+\frac{m\omega_c}{2\hbar}(y-ix)\Big\}\Big]|\psi_2\rangle=\varepsilon|\psi_1\rangle\,,\end{aligned} \tag{6}$$

$$\begin{aligned}\Big[ &-\frac{\hbar^2}{2m}(\partial_x^2+\partial_y^2+\partial_z^2)+\frac{1}{8}m\omega_c^2(x^2+y^2)-\frac{i\hbar\omega_c}{2}(-y\partial_x+x\partial_y)+V(x,y,z)\\ &+eE_z z+\frac{1}{2}g_0\mu_B B\sigma_z\Big]|\psi_2\rangle+\Big[\alpha_R eE_z\Big\{-\partial_x+i\partial_y+\frac{m\omega_c}{2\hbar}(x+iy)\Big\},\\ &+\alpha_D\Big\{-i\partial_x+\partial_y+\frac{m\omega_c}{2\hbar}(y+ix)\Big\}\Big]|\psi_1\rangle=\varepsilon|\psi_2\rangle\,.\end{aligned} \tag{7}$$

where $\omega_c = eB/m$.

## 3. Computational Method

The geometry of GaAs conical QDs with wetting layer is shown in Fig. 1. The QDs are surrounded by host barrier material $Al_{0.3}Ga_{0.7}As$. We diagonalize the total Hamiltonian, H, using the finite-element method.[20] A typical representative geometry contains 56,729 elements. We impose Dirichlet boundary conditions at the outside boundaries to let the wave function to vanish and Neumann boundary conditions at the internal boundaries to let the wave function to follow continuity assumptions. Then, we find eigenvalues and eigenfunctions by solving two coupled equations (eigenvalue problem) (6) and (7) that let us analyze the effective $g$-factor of electrons with several control parameters such as electric and magnetic fields as well as lateral size of the QDs. The material parameters for modeling of AlGaAs/GaAs are taken from Table 1.

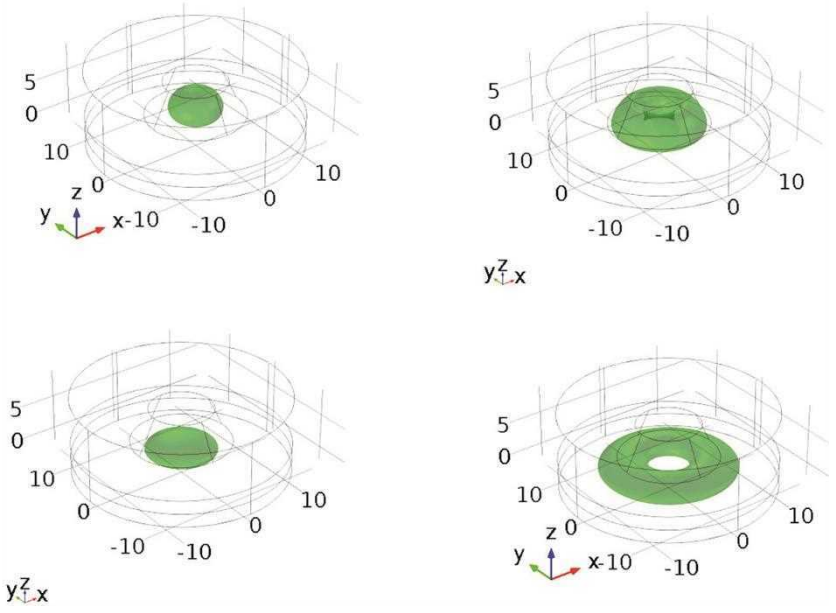


Fig. 1. (Color online) Lowest spin and orbital states wave functions of electrons in conical GaAs/AlGaAs QDs at $E_z = 0.001$ V/nm (upper panel) and $E_z = 0.1$ V/nm (lower panel). Evident penetration of the wave function from the QD region to the barrier material provides the variation in the Landé $g$-factor of electrons that can be utilized to design spintronic devices.

## 4. Results and Discussions

In Fig. 1, we have plotted probability distribution ($|\psi_1|^2 + |\psi_2|^2$ (arbitrary unit)) of ground (left panel) and first excited state (right panel) wave functions of electrons at $E_z = 0.001$ V/nm (upper panel) and $E_z = 0.1$ V/nm (lower panel). As we can see, the penetration of electron wave function into the barrier material is enhanced for larger values of the applied electric field along $z$-direction. This leads to the variation in the effective $g$-factor (see also Figs. 2 and 3) in GaAs/$Al_{0.3}Ga_{0.7}As$ QDs of electron that can be utilized to design spin current "ON" and "OFF" for in quantum information processing and other applications.[23] In Fig. 3 (upper panel), we have plotted effective $g$-factor, $g = (\varepsilon_1 - \varepsilon_2)/\mu_B B$ (absolute value) of electrons versus electric fields. Here, the variation in the effective $g$-factor of electrons of QDs with electric field can be seen and can be applied to make quantum logic gates for

Table 1. The material constants used in our calculations have been taken from Refs. 17–19.

| Parameters | GaAs | $Al_{0.3}Ga_{0.7}As$ |
|---|---|---|
| $g_0$ | $-0.44$ | 0.4 |
| $m$ | $0.067m_0$ | $0.088m_0$ |
| $\alpha_R$ [nm$^2$] | 0.044 | 0.022 |
| $\alpha_D$ [eV nm$^3$] | 0.026 | 0.0076 |

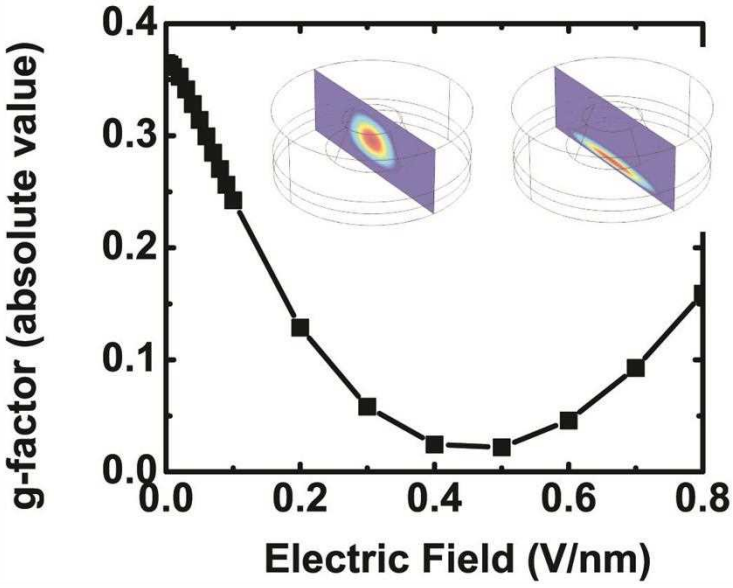


Fig. 2. (Color online) Effective $g$-factor of electrons versus externally applied electric field, $E_z$ in conical GaAs/AlGaAs QDs at $B = 0.5$ T. Variation in the Landé $g$-factor of electrons can be seen due to the penetration of QD electron wave function (see inset plots (left for $E_z = 0.001$ V/nm and right for $E_z = 0.8$ V/nm)) into the barrier material, AlGaAs, that can be utilized to design quantum switches for spintronic devices.

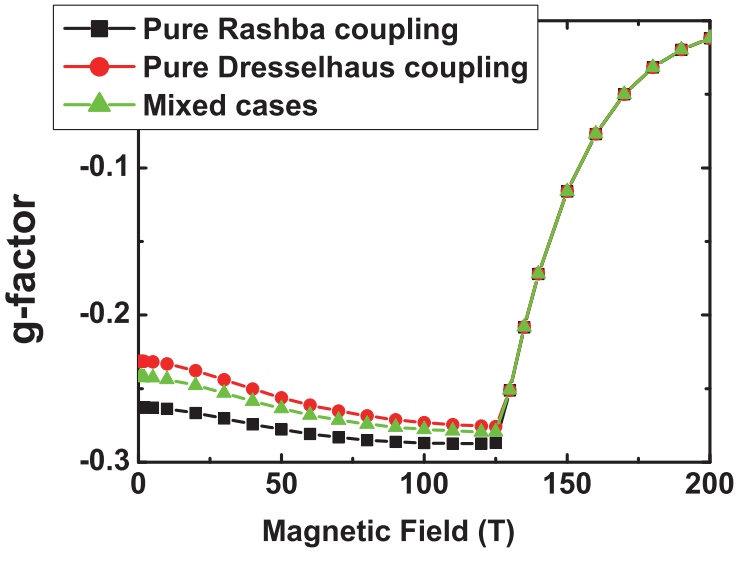


Fig. 3. (Color online) Tuning $g$-factor of electrons with magnetic field in conical GaAs QDs at $E_z = 0.1$ V/nm. Variation in the Landé $g$-factor of electrons can be seen for the pure Rashba, pure Dresselhaus and mixed spin–orbit coupling cases that can be utilized to design quantum switches for spintronic devices.

such applications as spintronic devices. At large electric fields, we find the vanishing $g$-factor of electrons which tells that the Bloch wave functions of electrons exactly reside at the heterojunction. By increasing applied electric field along $z$-direction, the Bloch wave funcution of electrons penetrate into the AlGaAs region and thus we find positive values of effective $g$-factor. The Rashba and Dresselhaus spin–orbit coupling coefficients become equal at $E_z \approx 0.3$ V/nm (see Ref. 6) which immediately leads to the conclusion that the Rashba spin–orbit coupling is a dominating factor to let the effective $g$-factor vanish. In Fig. 3, we have plotted the effective $g$-factor of electrons versus magnetic field in $GaAs/Al_{0.3}Ga_{0.7}As$ QDs for the pure Rashba, pure Dresselhaus and mixed spin–orbit coupling cases to see the interplay between these spin–orbit couplings. Here we see that the effective $g$-factor of electrons for the mixed spin–orbit coupling lies between for the corresponding values for the case of the pure Rashba and pure Dresselhaus spin–orbit couplings. This means that for the pure Rashba case, the Bloch wave functions of electrons mainly reside in the GaAs region and slightly penetrate towards the AlGaAs region for the pure Dresselhaus spin–orbit coupling case. The interplay between the Rashba and Dresselhaus spin–orbit couplings induces smaller range of $g$-factor tuning compared to the pure Rashba case and larger $g$-factor tuning compared to the pure Dresselhaus spin–orbit coupling in $GaAs/Al_{0.3}Ga_{0.7}As$ conical QDs. At large magnetic fields in Fig. 3, we find the level crossing due to an admixture of spin and orbital states of electrons in $GaAs/Al_{0.3}Ga_{0.7}As$ conical QDs.

## 5. Conclusion

We have provided three-dimensional results on the tuning of the effective $g$-factor of electrons with spin–orbit coupling in $GaAs/Al_{0.3}Ga_{0.7}As$ conical QDs and shown that the level crossing can be observed at large magnetic fields ($B \approx 125$ T) due to the admixture of the spin and orbital states of the electrons in such QDs. In Fig. 2, we have demonstrated that the penetration of electron wave function into the barrier material is enhanced for larger values of the applied electric field along $z$-direction. This leads to the variation in the effective $g$-factor of electrons that can be utilized to design spin current "ON" and "OFF" for applications in straintronic devices. In Fig. 3, we have shown that the interplay between the Rashba and Dresselhaus spin–orbit couplings induce smaller range of $g$-factor tuning compared to the pure Rashba case and larger $g$-factor tuning compared to the pure Dresselhaus spin–orbit coupling. The reported results provide further insight into physical phenomena critical for the design spintronic devices for quantum logic gates, quantum switches and other optoelectronic devices for application in quantum computing and quantum information processing.

## Acknowledgments

This work has been supported by NSERC and CRC programs (Canada). R. M. was supported by the Natural Sciences and Engineering Research Council (NSERC) of

Canada, the Canada Research Chair (CRC) program, and the Bizkaia Talent Grant under the Basque Government through the BERC 2014-2017 program, as well as Spanish Ministry of Economy and Competitiveness MINECO: BCAM Severo Ochoa excellence accreditation SEV-2013-0323.

## References

1. D. V. Bulaev and D. Loss, *Phys. Rev. Lett.* **95**, 076805 (2005).
2. D. V. Bulaev and D. Loss, *Phys. Rev. B* **71**, 205324 (2005).
3. J. M. Elzerman *et al.*, *Nature* **430**, 431 (2004).
4. M. Kroutvar *et al.*, *Nature* **432**, 81 (2004).
5. S. Prabhakar and J. E. Raynolds, *Phys. Rev. B* **79**, 195307 (2009).
6. S. Prabhakar *et al.*, *Phys. Rev. B* **82**, 195306 (2010).
7. S. Prabhakar, R. Melnik and L. Bonilla, *Phys. Rev. B* **89**, 245310 (2014).
8. S. Prabhakar and R. Melnik, *Eur. Phys. J. B* **88**, 273 (2015).
9. S. Takahashi *et al.*, *Phys. Rev. Lett.* **104**, 246801 (2010).
10. A. V. Khaetskii and Y. V. Nazarov, *Phys. Rev. B* **61**, 12639 (2000).
11. Y. A. Bychkov and E. I. Rashba, *J. Phys. C: Solid State Phys.* **17**, 6039 (1984).
12. G. Dresselhaus, *Phys. Rev.* **100**, 580 (1955).
13. R. Sousa and S. Sarma, *Phys. Rev. B* **68**, 155330 (2003).
14. C. E. Pryor and M. E. Flatté, *Phys. Rev. Lett.* **96**, 026804 (2006).
15. C. E. Pryor and M. E. Flatté, *Phys. Rev. Lett.* **99**, 179901 (2007).
16. M. P. Nowak *et al.*, *Phys. Rev. B* **83**, 245324 (2011).
17. S. Prabhakar, R. Melnik and L. L. Bonilla, *Phys. Rev. B* **87**, 235202 (2013).
18. P. von Allmen, *Phys. Rev. B* **46**, 15382 (1992).
19. F. S. Stern and S. Sarma, *Phys. Rev. B* **30**, 840 (1984).
20. Comsol Multiphysics version 5.1 (www.comsol.com).
21. S. Prabhakar, J. E. Raynolds and R. Melnik, *Phys. Rev. B* **84**, 155208 (2011).
22. S. Prabhakar, R. Melnik and A. Inomata, *Appl. Phys. Lett.* **104**, 142411 (2014).
23. H. W. Jiang and E. Yablonovitch, *Phys. Rev. B* **64**, 041307 (2001).